DALTON
FULL PAPER

Spontaneous magnetization below 7.7 K based on an extended 3-D H-bonding network material: synthesis, crystal structure and magnetic properties

Xiaoming Ren,*[a,b] Youcun Chen,[a] Cheng He[c] and Song Gao*[c]

[a] *Department of Chemistry, Anqing Normal College, Anqing 246011, P. R. China*
[b] *Max-Planck-Institut für Festkörperforschung, Heisenbergstrasse 1, Postfach 800665, D-70569 Stuttgart, Germany*
[c] *State Key Laboratory of Rare Earth Materials Chemistry and Applications, Peking University, Bejing 100871, P. R. China*

Received 20th May 2002, Accepted 1st August 2002
First published as an Advance Article on the web 13th September 2002

The structure of the complex [4-aminopyridinium][Ni(mnt)$_2$], as determined by X-ray single crystal analysis, consists of 4-aminopyridinium cations and [Ni(mnt)$_2$]$^-$ anions. The interactions between anions and cations *via* the bifurcated N(Py)–H···NC H-bonds give rise to a 1-D zigzag chain of alternating cations and anions, and a 3-D H-bonding network through further N(NH$_2$)–H···NC interactions. χ_{dc} and χ_{ac} have been measured down to 1.8 K and analysed, indicating the existence of a spin canting phenomenon. Below the critical temperature (around 7.7 K), the sample spontaneously magnetizes, and the hysteresis loop was observed at 1.85 K, corresponding parameters are as follows: H_c = 150 Oe and M_r = 7.9 emu mol^{-1}. The pathway of the exchange interaction in this complex *via* H-bonding is discussed in light of the crystal structure analysis.

Introduction

In recent years, the principles of supramolecular chemistry, in which a great deal of new concepts concern intermolecular non-covalent interactions such as H-bonding and π–π stacking interactions, have been introduced into the area of materials science,[1] and some have yielded materials exhibiting novel properties.[2]

The preparation of molecular based magnets *via* the association of paramagnetic complex molecules through H-bonding interactions have attracted wide interest.[3] However, in this field little attention has been paid to the construction of [M(mnt)$_2$]$^-$ [M = Ni(III), Pd(III) and Pt(III)] with pyridinium derivatives, in which the CN groups of the mnt^{2-} ligand and H–N of the pyridinium derivatives may undergo H-bonding interactions. Actually, our primary work showed that there are strong bifurcated H-bonding interactions between these blocks.[4] Therefore, we might obtain 2-D and 3-D molecular magnet based on this class of building block if a reasonable pyridinium derivative is chosen. In this contribution, we report on the synthesis, crystal structure and magnetic properties of a molecular based magnet, [4-aminopyridinium][Ni(mnt)$_2$], with an extended 3-D H-bonding network.

Experimental

Materials

Disodium maleonitriledithiolate (Na$_2$mnt) was prepared following the procedure reported in the literature.[5] The pyridinium chloride derivative was prepared by reaction between pyridine derivative and one equivalent of dilute hydrochloric acid. A similar method to that reported for the synthesis of [Bu$_4$N]$_2$[Ni(mnt)$_2$][5] was used to prepare [4-aminopyridinium]$_2$[Ni(mnt)$_2$].

Synthesis of [4-aminopyridinium][Ni(mnt)$_2$] (1)

A MeCN solution (10 cm^3) of I$_2$ (150 mg, 0.59 mmol) was slowly added to a MeCN solution (10 cm^3) of [4-aminopyridinium]$_2$[Ni(mnt)$_2$] (530 mg, 1.0 mmol) and the mixture was stirred for 20 min. MeOH (80 cm^3) was then added, and the mixture allowed to stand overnight; the 374 mg of microcrystals formed were filtered off, washed with MeOH and dried *in vacuo* (86% yield). Elemental analysis: calc. for NiC$_{13}$H$_7$N$_6$S$_4$: C, 35.96; H, 1.63; N, 19.36. Found: C, 35.81; H, 1.72; N, 19.28%. IR (cm^{-1}): 3357.1s (ν_{N-H}), 3234.5s (ν_{N-H}), 2212.6vs ($\nu_{C\equiv N}$), 1604.0s ($\nu_{C\equiv N}$), 1475.7m ($\nu_{C=C}$), 1429.1m ($\nu_{C=C}$), 873.4w (ν_{C-S}).

Physical measurements

Elemental analyses were performed using a Perkin-Elmer 240 analytical instrument. IR spectra were obtained with KBr pellets in the 4000–400 cm^{-1} region, using an IFS66 VFT–IR spectrophotometer. Magnetic susceptibility was determined in the temperature range 2–285 K on a MagLab system 2000 magnetometer, and diamagnetism was corrected by Pascal's constants (2.0×10^{-4} emu mol^{-1}). The ESR spectra were recorded with a polycrystalline sample on a (JEOL) JES-1XG spectrometer at 100 kHz modulation at room temperature. Mn^{2+} in MgO was used as a standard sample (ESR marker).

Data collection, structure solution and refinement

A brown–red single crystal with dimensions of 0.3 × 0.2 × 0.2 mm was mounted on a Siemens SMART CCD area detector with monochromated Mo-Kα radiation at room temperature. Crystal data collection parameters and refinement details are listed in Table 1. All computations were carried out *via* a PC-586 computer using the SHELXTL-PC program package.[6] The structure was solved by direct methods and refined on F^2 by full-matrix least-squares methods. All the non-hydrogen atoms were refined anisotropically. Hydrogen atoms were placed in their calculated positions and refined following the riding model.

CCDC reference number 179243.

See http://www.rsc.org/suppdata/dt/b2/b204902c/ for crystallographic data in CIF or other electronic format.

Table 1 Crystal data and structure refinement for **1**

Empirical formula	$C_{13}H_7N_6NiS_4$
Formula weight	434.20
T/K	293(2)
Wavelength/Å	0.71073
Crystal system	Monoclinic
Space group	$C2/c$
a/Å	41.3120(10)
b/Å	6.4570(10)
c/Å	12.9580(10)
β/°	93.730(10)
Volume/Å^3	3449.2(6)
Z	8
Absorption coefficient/mm^{-1}	1.616
F(000)	1752
Crystal size/mm^3	0.3 × 0.2 × 0.2
Reflections collected	8385
Independent reflections	3034 [R(int) = 0.0626]
Refinement method	Full-matrix least-squares on F^2
Data/restraints/parameters	3034/0/220
Goodness-of-fit on F^2	1.092
Final R indices [$I > 2\sigma(I)$]	$R1$ = 0.0510, $wR2$ = 0.1496
R indices (all data)	$R1$ = 0.0543, $wR2$ = 0.1525

Results and discussion

Description of the structure

Complex **1** crystallizes in monoclinic space group $C2/c$. An ORTEP view with non-hydrogen atom labeling is shown in Fig. 1. There are two halves of non-equivalent $[Ni(mnt)_2]^-$

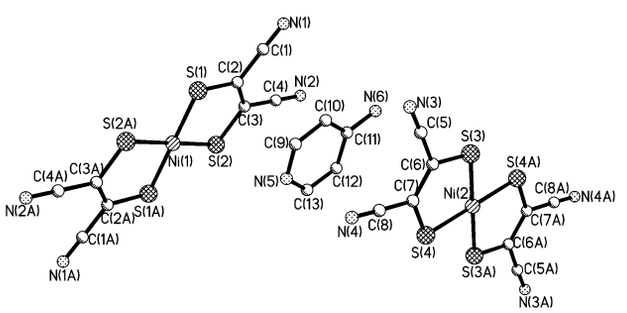

Fig. 1 ORTEP[14] view of **1** with atom labeling. Hydrogen atoms are omitted for clarity.

anions and a [4-aminopyridinium]$^+$ cation in the asymmetric unit cell. For two $[Ni(mnt)_2]^-$ anions, the Ni(1) and Ni(2) atoms are coordinated to four sulfur atoms and exhibit square-planar coordination geometry, respectively. The average Ni–S bond distances are 2.1441(9) Å in the anion containing the Ni(1) atom and 2.1457(9) Å in the anion containing the Ni(2) atom. The bond angles within the five-membered ring are 92.82(4)° for S(1)–Ni(1)–S(2) and 93.92(4)° for S(3)–Ni(2)–S(3). These results agree well with those found in $[Ni(mnt)_2]^-$ complexes.[4] The anion containing the Ni(2) atom is almost planar, and all deviations from the four sulfur atoms are less than 0.06 Å. However, the CN groups for the anion containing the Ni(1) atom are bent away from the coordination plane defined by the four sulfur atoms, and the deviations are 0.125 Å for the N(1) atom and 0.124 Å for the N(2) atom, respectively.

There are three H-bonding donors for 4-aminopyridinium, and four H-bonding acceptors for $[Ni(mnt)_2]^-$; H-bonding interactions are thus expected between the anions and cations. Actually, the two types of strong H-bonding interactions observed in **1** are as depicted in Fig. 2, one exists between the N atoms of the NH_2 groups and the N atoms of the CN groups of the mnt^{2-} ligands, and another bifurcated H-bonding between the N–H of the pyridinium and the CN groups of the mnt^{2-} ligands which is observed in some bipyridinium-containing compounds.[7] The corresponding distances and angles of H-

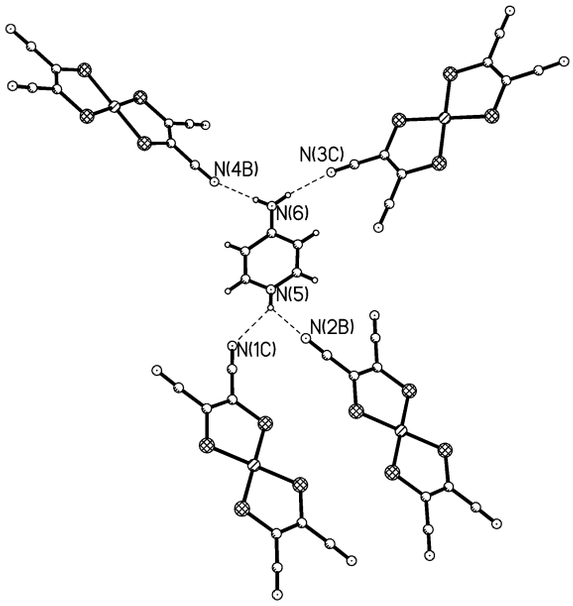

Fig. 2 H-bonding interactions between anions and cations for **1**.

bonding contacts are summarized in Table 2. The bifurcated H-bonding interactions between the CN groups and N–H of the pyridiniums give rise to a zigzag chain of alternating cations and anions, and the H-bonding interactions between the CN groups and the amino groups result in this complex forming an extended 3-D H-bonding network. The packing diagrams for **1** viewed down the a- and c-axes are displayed in Figs. 3

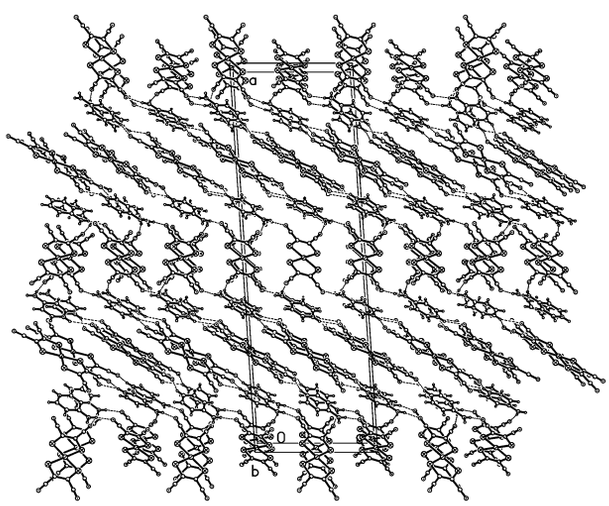

Fig. 3 Extended H-bonding network viewed down the a-axis, and showing two types of channels for **1**.

and 4, respectively. Two types of channel are clearly shown in Fig. 3. The shortest Ni···Ni, Ni···S and S···S distances between neighboring $[Ni(mnt)_2]^-$ anions are 6.46, 4.86 and 3.81 Å. These distances are larger than the corresponding atom sums of van de Waals radii of 3.26, 3.48 and 3.7 Å, respectively,[8] so weak magnetic interactions between Ni(III) ions *via* Ni(III)···Ni(III) or Ni···S···Ni or Ni···S···S···Ni exchange pathways are expected.

Magnetic properties

Fig. 5a shows the variation of χ_m and $\chi_m T$ with temperature for **1** measured in a field of 10 kOe, where χ_m denotes molar magnetic susceptibility and T temperature. The calculated $\chi_m T$ at 150 K, 0.224 emu K mol^{-1}, is less than the spin-only value

Table 2 Hydrogen bonds for **1** (Å and °)

D–H···A	*d*(D···H)	*d*(H···A)	*d*(D···A)	(DHA)
N(5)–H(5A)···N(1)#3	0.86	2.35	3.030(5)	135.7
N(5)–H(5A)···N(2)#4	0.86	2.36	3.039(5)	136.6
N(6)–H(6A)···N(4)#5	0.86	2.17	3.019(5)	168.1
N(6)–H(6B)···N(3)#6	0.86	2.17	3.023(5)	170.4

Symmetry transformations used to generate equivalent atoms: #1: $-x + 1/2, -y + 1/2, -z + 1$; #2: $-x + 1, -y, -z + 1$; #3: $x, -y + 1, z + 1/2$; #4: $x, -y, z + 1/2$; #5: $x, y - 1, z$; #6: $x, -y + 1, z - 1/2$.

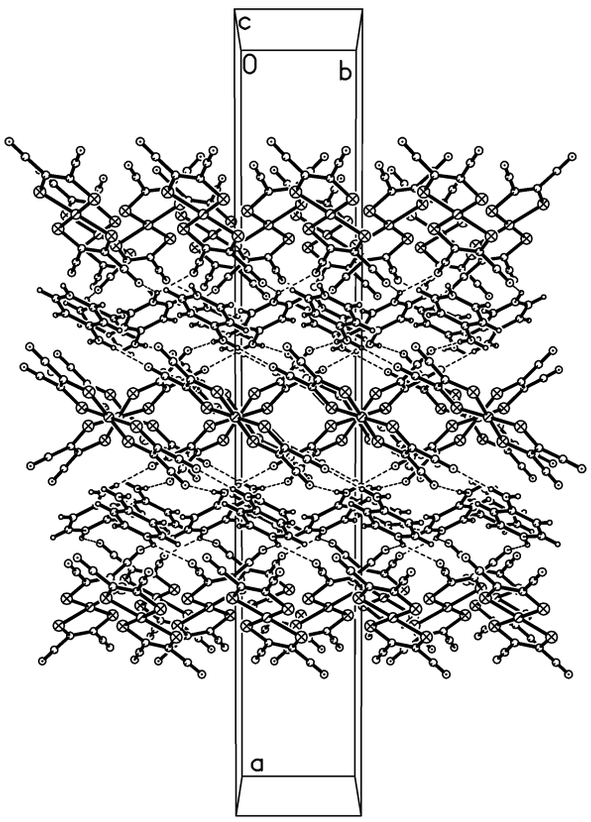

Fig. 4 Extended H-bonding network viewed down the *c*-axis.

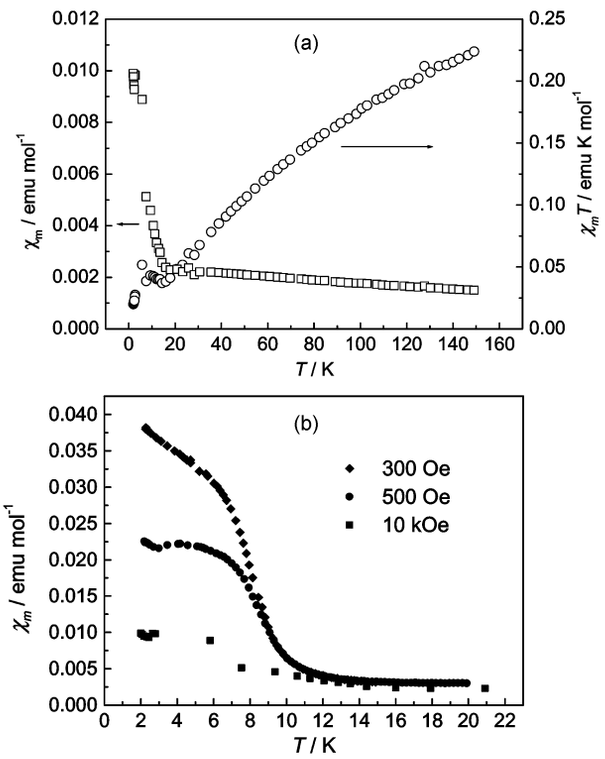

Fig. 5 (a) Variation with temperature of χ_m and $\chi_m T$ for **1** (dc field 10 kOe), and (b) the plots of χ_m at three values of applied field.

expected for one non-interacting $S = 1/2$ (0.375 emu K mol^{-1}). The $\chi_m T$ value decreases as the sample temperature decreases, and the result indicates that there exist antiferromagnetic coupling interactions between neighboring Ni(III) ions. It is noteworthy that the χ_m *versus* T curve undergoes an inflection around 16 K, and the χ_m values depend on the external magnetic field below this temperature (as shown in Fig. 5b). This transition around 16 K may suggest that there is ferromagnetic ordering for **1** in the lower-temperature range.[9,10]

To confirm the appearance of magnetic ordering and determine the precise critical temperature, ac magnetic susceptibility measurements were performed. Typically, in a magnet containing net magnetic moments in the ordered state (for example, ferromagnet, ferrimagnet, or canted antiferromagnet), these measurements show a maximum in the in-phase signal (χ') near T_c and the out-of-phase signal (χ'') starts to appear at temperatures just below T_c. In **1**, χ' shows a maximum around 7.7 K indicating that the magnetic ordering may occur near this temperature, and a non-zero χ'' was not observed below 7.7 K. In order to gain a deeper insight into the low-temperature magnetic behavior of **1**, we performed χ_{ac} measurements as a function of temperature at different frequencies, and found the maximum of χ' is independent on the frequency of ac field, although χ'' signals are very weak which indicates that the ferromagnetic component is small due to very weak canting (Fig. 6). The FCM and ZFCM measurements (in a 300 Oe measured field) from 1.8 to 15 K for **1** show evidence of magnetic ordering, and a small but clear remnant magnetization is observed below ~7.7 K (Fig. 7). These results confirm long-range ordering is present.

Further magnetization measurements for **1** show a hysteresis loop with $H_c = 150$ Oe and $M_r = 7.9$ emu mol^{-1} at 1.85 K (as shown in the inset of Fig. 8). When the external magnetic field reaches 6 T, the magnetic moment is only 0.042 μ_B, and significantly lower than that anticipated for a purely ferromagnetic material (Fig. 8). This weak ferromagnetism of **1** at low temperature may arise from a consequence of canted spin antiferromagnetism. The mechanism for spin canting requires that the canted spins in the solid state are not related by a center of inversion. Spin canting arises through a Dzyaloshinsky–Moriya interaction,[11–13] which minimizes the coupling energy when two spins are perpendicular to one another, and this magnitude is proportional to $\Delta g/g$. The ESR spectrum of a polycrystalline sample measured at room temperature for **1** showed the anisotropic characterization, and g_1, g_2 and g_3 are found to be 2.136, 2.047 and 1.999 from ESR measurements. The results of the structural analysis of **1** indicate that a center of inversion is present in a *C*2/*c* space group; the antisymmetric exchange is excluded as a factor accounting for the spin canting so only the local anisotropy (non-compensation of the local *g* values in the structure) would account for the canting observed.

Conclusions

A new system containing $[Ni(mnt)_2]^-$ anions has been structurally characterized and its magnetic behavior investigated.

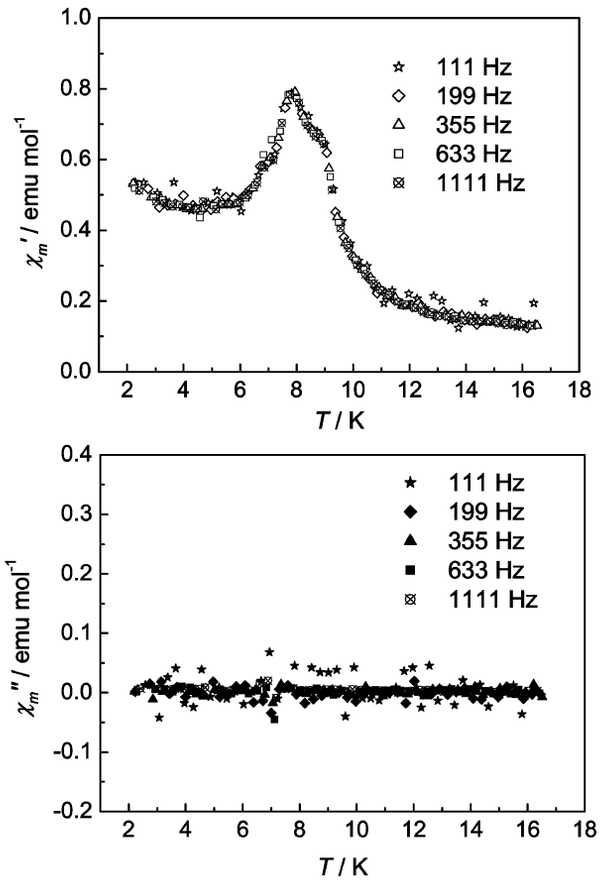

Fig. 6 Temperature dependence of ac magnetic susceptibility measured at different frequencies, (Top: real part; Bottom: imaginary part).

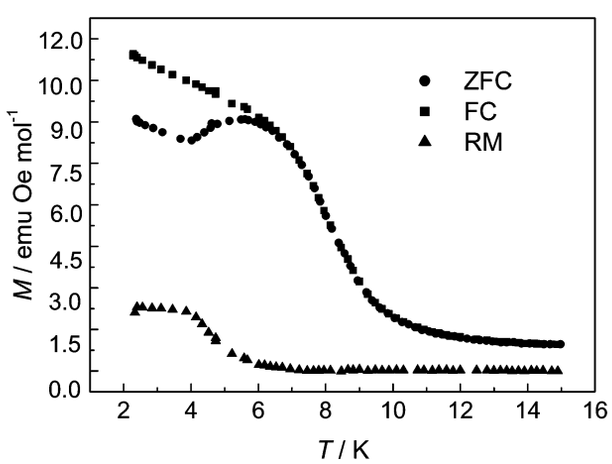

Fig. 7 Magnetization of **1** cooled in zero-field (ZFCM), a field of 300 Oe (FCM) and remnant magnetization (RM), respectively.

The H-bonding interactions between anions and cations give extended three-dimensional H-bonding networks. To the best of our knowledge, reports of the mnt^{2-} ligand acting as a H-bonding acceptor are rare. The various magnetic data for **1** are consistent with antiferromagnetic coupling between neighboring Ni(III) ions with long-range ferromagnetic ordering below 7.7 K. We interpret these magnetic properties as a consequence of canted spin antiferromagnetism leading to weak ferromagnetism at low-temperature.[9,10] The analysis of the crystal structure of **1** indicated the shortest contacts of Ni···Ni, Ni···S and S···S between neighboring $[Ni(mnt)_2]^-$ anions are significantly larger the sums of the van de Waals radii of corresponding atoms, a magnetic exchange mechanism

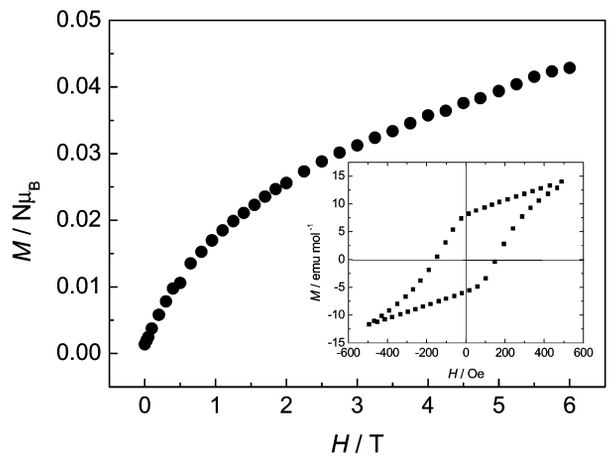

Fig. 8 Magnetization curve obtained at 1.85 K for **1**. The inset shows the magnetic hysteresis loop with H_c = 150 Oe and M_r = 7.9 emu mol^{-1} at 1.85 K.

for **1** could thus involve interactions *via* the H-bonding network linking $[Ni(mnt)_2]^-$ anions.

Acknowledgements

The authors are grateful for the financial support of the National Natural Science Foundation of China (project no. 20171001 and 20125104), and the Natural Science Foundation of Anhui Province of China (project no. 01012038).

References

1 (*a*) H. Saadeh, L. Wang and L. Yu, *J. Am. Chem. Soc.*, 2000, **122**, 546; (*b*) D. S. Lawrence, T. Jiang and M. Levett, *Chem. Rev.*, 1999, **95**, 2229.
2 (*a*) G. B. Gardner, D. Venkataraman, J. S. Moore and S. Lee, *Nature*, 1995, **374**, 792; (*b*) D. Venkataraman, G. B. Gardner, S. Lee and J. S. Moore, *J. Am. Chem. Soc.*, 1995, **117**, 11600; (*c*) M. Fujita, Y. J. Kwon, S. Washizu and K. Ogura, *J. Am. Chem. Soc.*, 1994, **116**, 1151; (*d*) O. M. Yaghi, G. Li and H. Li, *Nature*, 1995, **378**, 703.
3 (*a*) Y. Pontillon, T. Akita, A. Grand, K. Kobayashi, E. Lelievre-Berna, J. Pécaut, E. Ressouche and J. Schweizer, *J. Am. Chem. Soc.*, 1999, **121**, 10126; (*b*) A. Fragoso, M. L. Kahn, A. Castineiras, J.-P. Shtter, O. Kahn and R. Cao, *Chem. Commun.*, 2000, 1547; (*c*) D. G. Munno, D. Viterbo, A. Caneshi, L. Francese and M. Julve, *Inorg. Chem.*, 1994, **33**, 1585; (*d*) D. G. Munno, W. Ventura, G. Viau, L. Francese and M. Julve, *Inorg. Chem.*, 1998, **37**, 1458; (*e*) V. N. Ikorskii, V. I. Ovcharenko, Y. J. Shvedenkov, G. V. Romanenko, S. V. Fokin and R. Z. Sagdeev, *Inorg. Chem.*, 1998, **37**, 4360.
4 X. M. Ren, C. S. Lu, P. H. Wu and Q. J. Meng, *J. Chem. Crystallogr.*, 2002, **32**, 173.
5 A. Davison and H. R. Holm, *Inorg. Synth.*, 1967, **10**, 8.
6 G. M. Sheldrick, SHELXTL, Structure Determination Software programs, version 5.10, Bruker Analytical X-Ray Systems Inc., Madison, WI, USA, 1997.
7 A. L. Gillon, A. G. Orpen, J. Starbuck, X. M. Wang, Y. Rodríguez-Martín and C. Ruiz-Pérez, *Chem. Commun.*, 1999, 2287.
8 J. A. McCleverty, *Prog. Inorg. Chem.*, 1968, **10**, 49.
9 (*a*) S. J. Rettig, R. C. Thompson, J. Trotter and S. Xia, *Inorg. Chem.*, 1999, **38**, 1360; (*b*) S. J. Rettig, J. V. Sánchez, A. Storr, R. C. Thompson and J. Trotter, *J. Chem. Soc., Dalton Trans.*, 2000, 3931.
10 S. R. Batten, P. Jensen, C. J. Kepert, M. Kurmoo, B. Moubaraki, K. S. Murray and D. J. Price, *J. Chem. Soc., Dalton Trans.*, 1999, 2987.
11 (*a*) O. Kahn, *Molecular Magnetism*, VCH publisher, New York, 1993; (*b*) R. L. Carling, *Magnetochemistry*, Springer, Berlin, 1989.
12 A. J. Banister, N. Bricklebank, I. Lavender, J. M. Rawson, C. I. Gregory, B. K. Tanner, W. Clegg, M. R. J. Elsegood and F. Palacio, *Angew. Chem., Int. Ed. Engl.*, 1996, **35**, 2533.
13 N. Robertson, C. Bergemann, H. Becker, P. Agarwal, S. R. Julian, R. H. Friend, N. J. Hatton, A. E. Underhill and A. Kobayashi, *J. Mater. Chem.*, 1999, **9**, 1713.
14 M. N. Burnett and C. K. Johnson, ORTEP-III, Report ORNL-6895, Oak Ridge National Laboratory, Oak Ridge, TN, 1996.